Multiple Beam Antenna Technology for Satellite Communications Payloads

(Invited Paper)

Sudhakar Rao, Minh Tang, and Chih-Chien Hsu
Lockheed Martin Commercial Space Systems
100 Campus Drive, Newtown, PA 18940
Email: sudhakar.rao@lmco.com

***Abstract*—**This paper reviews multiple beam antenna (MBA) technologies that are applicable for satellite communications payloads. It provides design, performance analysis, and hardware implementation aspects of various types of MBAs that include reflector MBAs, phased array MBAs, and lens MBAs. Parametric design of these MBAs and RF analysis for coverage gain and inter-beam isolation are given. Recent advances and trends in MBA technologies for space applications are discussed.

***Index Terms*—**Antenna arrays, lens antennas, multiple beam antennas, reflector antennas

I. INTRODUCTION

THERE has been a tremendous growth in the use of multiple beam antenna (MBA) payloads for both commercial and military communications satellites over the last decade [1-6]. MBAs are currently being used for direct broadcast satellites (DBS) such as EchoStar-X, DirecTV-4S, DirecTV-7S etc., personal communication satellites (PCS) such as Anik-F2, SpaceWay, CIEL-2, etc., mobile communications satellites such as ACeS, Thuraya, MSV, TerraStar, ONDAS, etc., military communications satellites such as WGS, MUOS, TSAT etc., and navigation satellites such as GPS-2, GPS-3, etc. These antenna systems for most cases provide a contiguous coverage of a geographical region as seen by the satellite by using high-gain multiple spot beams that provide downlink (satellite-to-ground) and uplink (ground-to-satellite) signals. Main advantages of the MBAs when compared to conventional contoured beam antennas are:

- Significantly higher antenna gain due to smaller size of the beam, resulting in improved effective isotropic radiated power (EIRP) for the downlink and improved gain-to-noise temperature (G/T) for the uplink,
- Increase in effective spectral bandwidth by several folds due to re-use of the frequency channels over several spot beams,
- Allows the use of much smaller ground terminals.

Fig. 1 illustrates typical contoured beam coverage and multiple beam coverage of the continental United States (CONUS) from a geo-stationary satellite. Contoured beam antenna shown in Fig. 1a has typical edge-of-coverage (EOC) gain of 30 dBi and has no frequency re-use (frequency re-use factor FRF is 1.0). The MBA shown in Fig. 1b has 68 overlapping spot beams arranged in a hexagonal grid lattice with an adjacent beam spacing of 0.52 degrees and beam diameter of 0.6 degrees at the triple-beam crossover point. The EOC gain is about 45 dBi (15 dB more than the contoured beam antenna) and has FRF of 17 with a 4-cell frequency re-use scheme. FRF is defined as the ratio of the number of beams to the number of frequency cells (typically 3, 4 or 7) per polarization. The multiple beams can be formed using either a single aperture or multiple aperture antennas and could use different frequency cell re-use schemes. Fig. 2 illustrates the

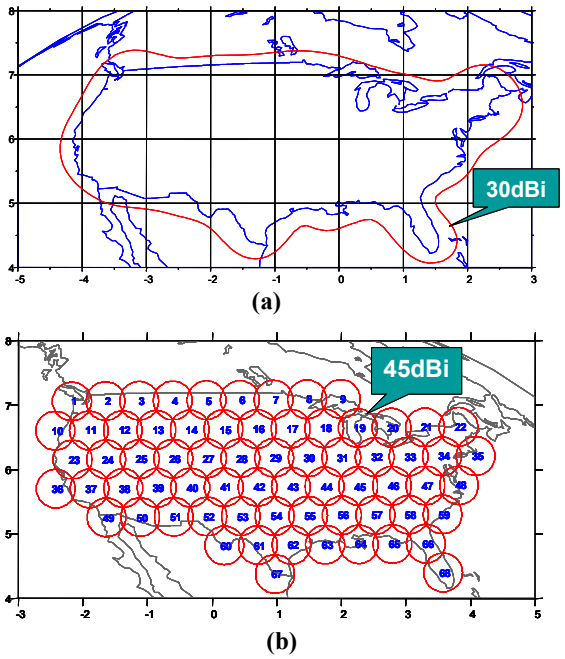

Fig. 1. Comparison of CONUS coverage beams with (a) conventional contoured beam antenna, and (b) multiple beam antennas (X-axis: Azimuth & Y-axis: Elevation).

aperture and frequency re-use concepts for MBAs. The aperture concepts include single, three, or four antenna apertures (reflectors or lenses), whereby adjacent beams are generated by different apertures and form an inter-leaved spot beam coverage on ground. The advantage of multiple aperture MBA is that it allows increasing the spacing between beams produced by the same aperture by a factor of 1.73 for a 3-aperture MBA and by a factor of 2.0 for a 4-aperture MBA.

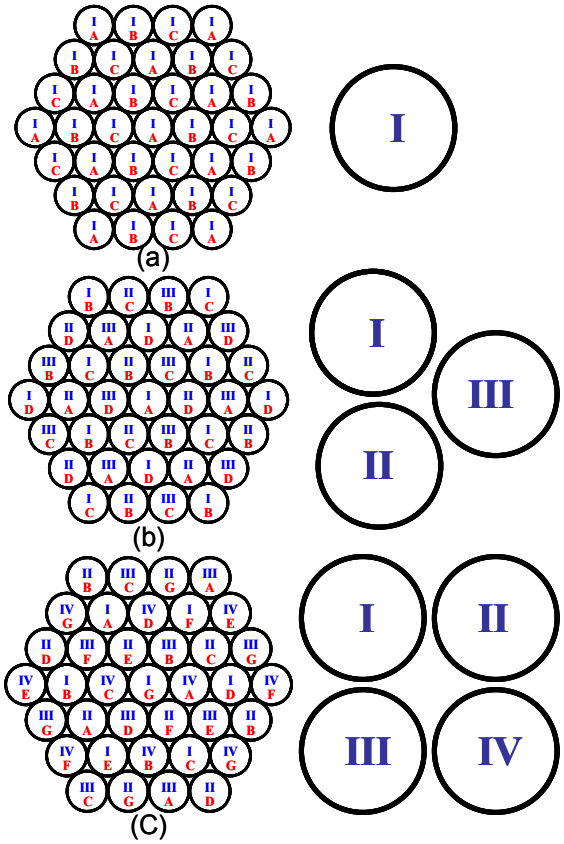

Fig. 2. Aperture and frequency re-use concepts for MBAs: (a) single-aperture MBA with 3-cell re-use scheme, (b) three-aperture MBA with 4-cell re-use, and (c) four-aperture MBA with 7-cell re-use.

The larger beam spacing allows increase in the feed horn size such that it optimally illuminates the reflector with increased beam EOC gain and reduced side lobe levels. Fig. 3 shows typical plot applicable to reflector or lens MBAs showing the impact of feed horn size (assuming single feed per beam without beam-forming networks) on the MBA performance. Single aperture MBAs have typical feed sizes of less than 1 wavelength and therefore have low efficiency values of around 45% and high sidelobes. On the other hand, a 4-aperture MBA has typical feed size of more than 2 wavelengths, resulting in antenna efficiency values of more than 75% and sidelobe levels of –25 dB. An increase in antenna gain of more than 2.2 dB and sidelobe improvement of about 8 dB are achieved with a 4-aperture reflector/lens

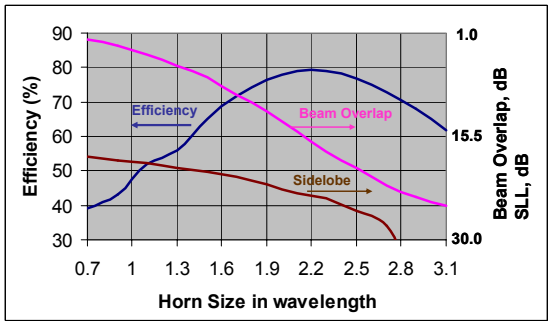

Fig. 3. MBA performance as a function of feed horn size.

MBA when compared to a single-aperture MBA (both employ single feed per beam). The main objectives of the MBA design are:

- Maximize the minimum coverage gain of each beam including pointing error,
- Minimize the gain loss due to beam scan effects,
- Maximize the aggregate co-polar isolation (C/I) among beams that re-use the same frequency,
- Maximize the cross-polar isolation (C/X) for each beam, and
- Maximize the beam congruency among uplink and downlink beams (for PCS, MSS applications).

The coverage region for most applications needs to be contiguously covered by the satellite with multiple spot beams. A hexagonal grid layout is usually preferred due to tight packing of the beams. The optimum beam diameter for circular coverage with uniform beams, total number beams, and adjacent beam spacing are given approximately as

$$\theta_0 = 0.6155\theta_c / N\,, \tag{1}$$

$$N_T = 1 + 3N(N+1)\,, \tag{2}$$

$$\theta_s = 0.866\theta_0 \tag{3}$$

where θ_0 is the beam diameter at triple-beam crossover level, N is the number of rings of the hexagonal layout excluding the central beam, N_T is the total number of beams, θ_c is the coverage diameter, and θ_s is the spacing between adjacent beams.

The typical beam layout of an MBA for global coverage from a geo-stationary satellite is shown in Fig. 4. It employs 91 overlapping spot beams with a hexagonal grid layout. The spacing between adjacent beams is 1.732 degrees and the beam diameter at triple beam cross-over is 2.0 degrees. Table 1 shows the

design variables for a global coverage with 17.6 degrees diameter.

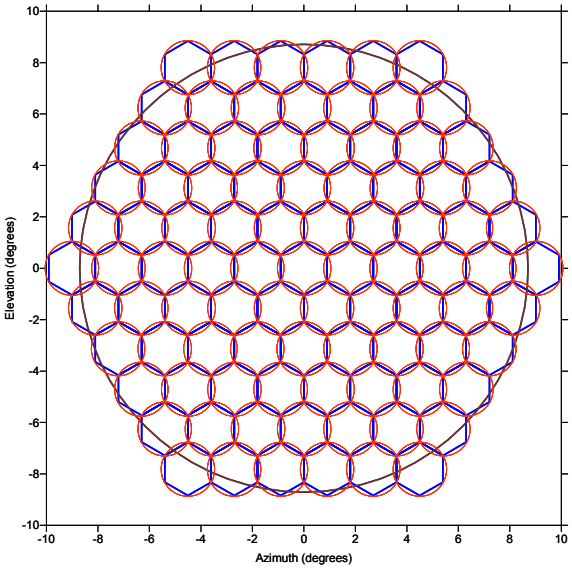

Fig. 4. Global coverage of an MBA with 91 over-lapping spot beams.

Table 1. Beam size versus number of beams for global coverage.

Beam Diameter	Beam Spacing	No. of Rings	Total No. of Beams
($?_0$)	($?_s$)	(M)	(M_T)
0.7	0.606	15	721
0.8	0.693	14	631
0.9	0.779	12	469
1.0	0.866	11	397
1.1	0.953	10	331
1.2	1.039	9	271
1.4	1.212	8	217
1.8	1.559	6	127
2.0	1.732	5	91
2.4	2.078	5	91
2.8	2.425	4	61

For national coverage with non-circular shape, the number of beams is obtained using the equation

$$N_T = 1.27 A_C / (\theta_s)^2 \qquad (4)$$

where A_C is the area of the coverage region in square degrees. Multiple beam antennas for satellite communications can be broadly classified into three categories: a) reflector MBAs, b) lens MBAs, and c) phased array MBAs. These three types of MBAs have been employed in the past for satellite communications. Both reflector and lens MBAs require feed arrays, where each beam is generated with single or multiple feeds. The phased array MBA employs the complete array to generate each beam. Waveguide lens MBAs have been used on DSCS III satellite [7, 8], but suffer from the disadvantages of limited bandwidth due to zoning of the lens to reduce mass, high mutual coupling among waveguide elements of the lens, and poor return loss. Dielectric lens MBAs are not preferred for space applications, especially for the transmit downlink, because of the electro-static discharge (ESD) and out-gassing associated with dielectric materials in vacuum. Reflector MBAs are most frequently used in the space industry due to their superior RF performance reduced mass, reduced cost, and mature technology. Multiple aperture reflector MBAs, where adjacent beams are generated from different apertures, are preferred over single reflector MBAs at higher frequencies such as Ku, Ka, and EHF bands where multiple reflectors (3 or 4) can be accommodated on the spacecraft. However, for mobile satellites at L-band and S-band frequencies, a single reflector MBA with beam-forming network is more commonly used due to spacecraft accommodation issues associated with large unfurlable mesh reflectors. Phased array MBAs have been developed mostly for military communications, where extensive on-orbit beam re-configurability is required. Details of these MBAs are given in the following sections.

II. REFLECTOR MBAS

Reflector MBAs are most commonly used for satellite communications due to better RF performance in terms of coverage gain and C/I, payload simplicity, reduced cost, and mature technology. These MBAs are classified into the following types: (a) single reflector with a single feed per beam, (b) single reflector with over-lapping feed clusters, and (c) multiple reflectors with single element per beam. The reflectors are typically offset-fed parabolic reflectors and the feed elements are usually horns. Type (a) requires electrically small feed horns of about one wavelength in diameter in order to achieve high adjacent beam overlaps, which result in gain values that are 2 dB to 3 dB lower than what could be achieved using optimal horn size as shown in Fig. 3 [1]. Type (b) design requires low-level beam-forming networks (LLBFNs where beams are formed before the high power amplifiers for transmit and after the low-noise amplifiers for receive) to provide element sharing among beams (typically shared among 7 beams) and beam combining functions (typically 7 elements used to form a beam). An advantage of LLBFN is that the network losses do not impact EIRP or G/T performance of the MBA. Type (b) MBA is typically used for mobile satellites at low frequencies such as L-band and S-band due to large physical sizes of the reflectors (larger than 5 meter) and feed arrays. These applications employ typically one large deployable mesh reflector and a feed array due to limitations of the spacecraft bus to accommodate multiple large reflectors. Type (c) employs multiple reflectors, each being illuminated with its own feed array, with three or four independent apertures. Each beam is generated

with a single feed horn of more than 2 wavelengths in diameter that provides optimal illumination on the reflector. Type (c) MBAs are used at Ku-band, Ka-band, and EHF, where smaller physical size of the reflector (typically less than 100 in. diameter) allows accommodation of multiple reflectors on the spacecraft.

a) Design and Analysis

Design and analysis of reflector MBAs are addressed in this section. Closed form equations are presented for the design of MBAs and their performance analysis, based on Gaussian beam representation of primary and secondary patterns. The beam parameters and the reflector parameters are shown in Fig. 5. Typical beam layout of a four-reflector MBA with 4-cell re-use scheme is shown in Fig. 5(a). The two "A" beams come from the same reflector in this example. It is to be noted that the feed horn size depends on the number of

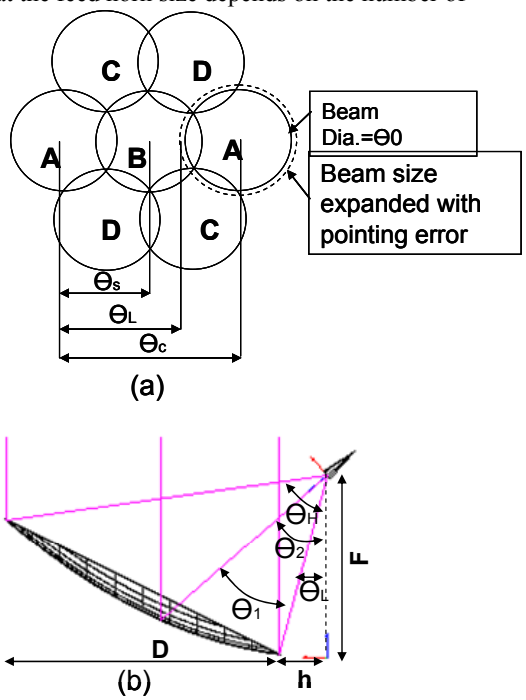

Fig. 5. (a) Beam Parameters with 4-aperture MBA with 4-cell re-use, and (b) Reflector Parameters.

reflectors used for the MBA and is independent of the frequency re-use scheme. The spacing between adjacent beam centers coming from the same reflector for a single reflector, 3-reflector, 4-reflector, and 7-reflector MBAs is given as

$$\theta_C^{1,3,4,7} = G^{1,3,4,7}\theta_s \ . \tag{5}$$

The constant G in the above equation is 1.0, 1.732, 2.0, and 2.646 for a single-reflector, 3-reflector, 4-reflector, and 7-reflector MBAs, respectively. The beam diameters shown in Fig. 5(a) need to be expanded with the satellite pointing error in order to evaluate the coverage gain and isolation into the re-use beams. The closest distance of the re-use beams from the beam peak is given by

$$\theta_L = \theta_C - 0.5\theta_0 - \Delta\theta^P \ . \tag{6}$$

The design of the MBA starts with the beam size requirements or the number of beams over a desired coverage region, and the frequency re-use plan. The beam size is defined as the diameter of the beam at the triple-beam crossover point, and is X dB below the beam peak (a typical value for X is about 4 dB). For a four-aperture MBA, the reflector size can be determined using the following equation

$$\theta_0^X = 65\left[\frac{X}{3}\right]^{0.5}\left(\frac{\lambda_L}{D}\right) \tag{7}$$

where θ_0^X is the full beam-width at X dB below beam peak, λ_L is the wavelength at the lowest frequency of the band, and D is the reflector diameter. The constants relating the beam-width to the normalized reflector size are 65.0, 75.0, and 83.9 for X=3, 4, and 5, respectively.

The focal-length to reflector diameter ration (F/D) depends on the coverage size and the maximum number of beam-widths scanned from the bore-sight direction. It also depends on the mechanical packaging issues on the spacecraft. For large scans (more than 4 beam-widths), a larger F/D ratio is desired to minimize the beam distortions caused by the coma lobes and to minimize gain loss due to scan. Typical F/D ratio for satellite antennas is in the range 1.0 to 1.6. The offset clearance h is selected such that the blockage-free condition is maintained for the maximum scanned beam, and is given approximately using the equation

$$h \geq 2F\tan\theta_{sm} \tag{8}$$

where θ_{sm} is the maximum scan angle towards the reflector offset from the bore-sight direction. The feed size and type of feed are the key design parameters for the MBAs. The feed diameter d_m depends on the beam spacing, number of apertures, and the reflector geometry, and is given as

$$d_m^{1,3,4,7} = G^{1,3,4,7}\theta_s / S_F \tag{9}$$

where S_F is the scan factor that depends on the reflector geometry and is given by:

$$S_F = \frac{1+X\left(\frac{D}{4F}\right)^2}{1+\left(\frac{D}{4F}\right)^2}\left[\frac{1+\cos\theta_2}{2F}\right] \tag{10}$$

and X = 0.30 for T < 6, and X = 0.36 for T > 6, and T is the feed illumination taper (positive dB) on the edge of

the reflector. The angular parameters θ_{l2} of the reflector geometry are given in [2].

The feed size and type of feed are critical to MBA design. For multiple-reflector MBA, the types of feeds applicable are Potter horns, high-efficiency horns, and corrugated horns. Corrugated horns are rarely used due to the thick walls required that make the electrical aperture smaller. Potter horns have broader beams and lower efficiency of about 70%. High-efficiency horns employ TE_{11}, TE_{12}, TE_{13}, etc. modes that make the aperture illumination uniform in both E-plane and H-planes and provide high efficiency values of up to 93% [5, 10]. The feed horn pattern can be modeled using a Gaussian beam representation which is given by

$$E(\theta) = \exp[-A(\theta/\theta_b)^2] \tag{11}$$

where θ_b is the half angle of the 3 dB beamwidth and is expressed as a function of efficiency as

$$\theta_b = [31 - 0.0041(93-\eta)^2 + 0.341(93-\eta)](\lambda/d_m) \tag{12}$$

where η is the efficiency of the feed horn. The feed illumination taper on the edge of the reflector T is given as

$$T = -20\log_{10}[\exp\{-0.3467(\theta_1/\theta_b)^2\}]. \tag{13}$$

The minimum coverage area directivity, taking into effect the scan loss, peak to edge gain variation of the beam, and the satellite pointing error is given as

$$D_C = 10\log_{10}\left[\left(\frac{\pi D}{\lambda_L}\right)^2 \eta_i\right] - GL(\delta_m) - B(\delta_m) - 10\log_{10}\left(\frac{0.5\theta_0^X + \Delta\theta^P}{0.5\theta_0^X}\right)^2 \tag{14}$$

where δ_m is the maximum number of beamwidths scanned from boresight, GL is the gain loss due to scan, and η_i is the antenna efficiency. GL and η_i are given as

$$GL(\delta) = \frac{0.0015\delta^2}{\left[(F/D_P)^2 + 0.02\right]^2} + \frac{0.011\delta}{\left[(F/D_P)^2 + 0.02\right]} \tag{15}$$

$$\eta_i = 4\cot^2(\theta_1/2)\left[1-\cos^n(\theta_1/2)\right]^2\left\{\frac{n+1}{n^2}\right\}\left[1.025 + 0.5119(\eta_f - 0.74) - 7.542(\eta_f - 0.74)^2\right] \tag{16}$$

and n is related to the feed taper as

$$n = \frac{-0.05T}{\log_{10}(\cos(\theta_1/2))}. \tag{17}$$

The 3 dB beamwidth of the reflector MBA at boresight and as a function of scan is given by

$$\theta_0^3 = (0.058T^2 + 0.171T + 58.44)(\lambda/D)$$

$$\theta_0^3(\delta) = \theta_0^3 10^{0.05GL(\delta)} \tag{18}$$

$$B(\delta_m) = X\left[\frac{\theta_0^X}{\theta_0^X(\delta_m)}\right]^2. \tag{19}$$

The copolar isolation (C/I) can be calculated by the power addition of all the J interfering beams that re-use the same frequency as the beam of interest and comparing with the directivity of the beam at any angular location of the coverage beam and is given as

$$C/I = D_C - 10\log_{10}\left[\left(\frac{\pi D}{\lambda}\right)^2 \eta_f\right] + \sum_{j=1}^{J}\left\{GL(\delta_j) + B_j\left(\frac{\theta_{js} + 0.5\theta_j - \Delta\theta^P}{0.5\theta_j}\right)^2\right\} \tag{20}$$

where θ_j is the diameter of jth interferer, and θ_{js} is the distance from the closest edge of the jth interferer to the beam of interest.

The C/I values are typically 10 dB, 13 dB, and 18 dB for a 3-cell, 4-cell, and 7-cell re-use schemes of the MBA.

b) Advanced Reflector MBA Technologies

This section describes some of the recent advances in reflector MBA technology. Fig. 6 illustrates evolution of reflector MBA technology. Configuration "A" is a conventional MBA employing separate set of reflectors for uplink and downlink frequency bands. The uplink reflectors are typically 1.5 times smaller than the downlink reflectors. Configuration "B" employs dual-band reflector antennas being fed with corrugated horns in order to reduce the number of apertures from 8 to 4. It suffers from reduced EOC gain and inferior C/I due to reduced efficiency of the feed (about 54% efficiency) caused by thick walls. The dual-band MBA (DMBA) configuration "C" overcomes the above limitations by employing smooth-walled dual-band high efficiency horns [5, 9, 10]. A novel MBA employing "stepped-reflector antenna" (SRA) technology, as illustrated in configuration "D" in Fig. 6, has been developed and patented by Lockheed Martin Commercial Space Systems (LMCSS) [4, 11]. It combines feed horn advancements with improved reflector technology in order to achieve significant performance improvements for future DMBAs. The high efficiency horns have been developed earlier for single narrow band applications, where desired higher order modes are generated with step discontinuities. In order to achieve

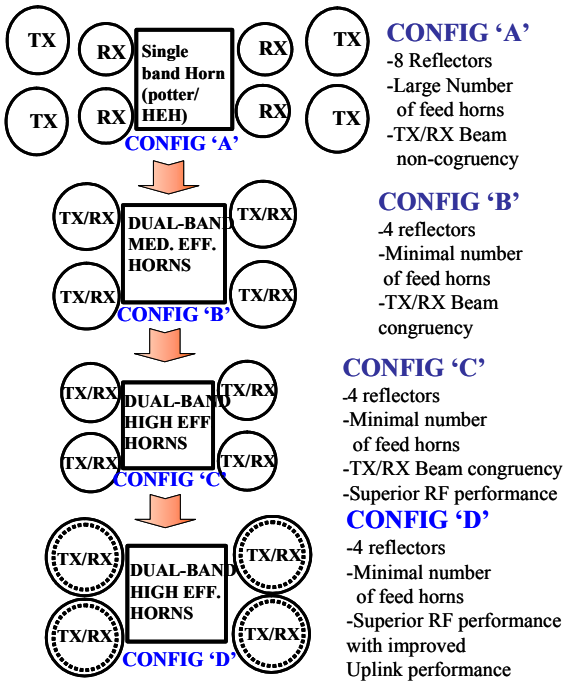

Fig. 6. Evolution of Reflector MBA Technology.

high efficiency values over both Tx and Rx bands of the DMBAs, a number of slope-discontinuities have been used to generate higher order $TE_{1,n}$ modes [10]. The horn geometry is synthesized using iterative analysis that employs mode-matching technique combined with a generalized scattering matrix (GSM) to evaluate the performance of the horn. Desired requirements for efficiency return loss, and cross-polar levels can be specified over both Tx and Rx frequencies and the synthesis method can be implemented by minimizing the cost function using mini-max optimization. Fig. 7 shows performance of a 2.27 in. diameter high-efficiency horn compared with a conventional corrugated horn. Both horns were used to evaluate detailed performance of a dual-band reflector with 80 in. reflector diameter, 116 in. focal length, and a 26 in. offset clearance. The reflector surface is shaped to broaden the Rx beam in both cases. Table 2 summarizes performance comparison of the DMBA with both types of horns. The DBHEH, when compared to a corrugated horn, improves EOC gain by about 0.9 dB at Tx and by about 2.0 dB at Rx, and improves C/I by about 3.0 dB.

DMBA configuration "D" developed by LMCSS includes use of the stepped-reflector antenna (SRA) technology to further improve the DMBA performance. The concept of SRA is illustrated in Fig. 8, where it employs outer annular region that are stepped and attached to the central portion of the reflector. Both central and annular stepped regions can be shaped to improve the RF performance and the transition region can be blended into the reflector to avoid abrupt discontinuities. The height h of the step is designed in conjunction with the DBHEH feed phase characteristics at the Rx frequencies in order to provide a 180-degree "phase reversal" at the step resulting a "flat-topped" Rx beams with significantly improved G/T.

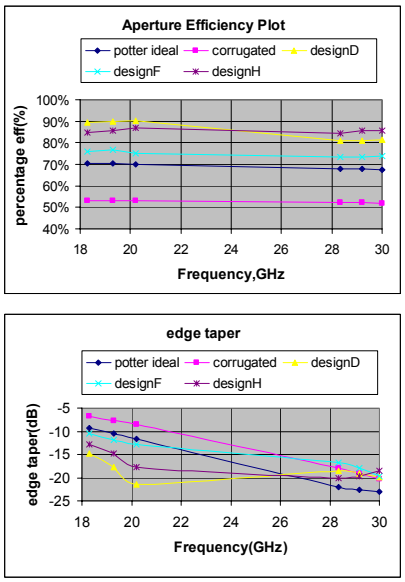

Fig. 7. Aperture efficiency and edge illumination taper comparison of various MBA horns.

Table 2. Performance Comparison of DMBAs "B" & "C" using conventional corrugated horns and DBHEH.

Performanc Paramete	CONVENTIONA HORN	HIGH EFF. DESIGN
	TX/RX	TX/RX
Efficiency, %	54 / 52	85 / 85
Edge Taper,	7/18	13 / 17
Primary C/X, dB	33 / 33	20 / 23
EOC Directivity, dBi	43.8 / 41.7	44.7 / 43.7
C/I, 3-cell (dB)	11.1 / 13.0	14.2 / 11.6
C/I, 4-cell (dB)	12.0 / 15.8	15.7 / 14.5
C/I, 7-cell (dB)	18.2 / 19.5	22.7 / 21.9
C/X, dB	30.0 / 28.0	21.0 / 20.0

The near-field phase distribution of the SRA is plotted in Fig. 9 and shows the desired 180-degree phase reversal near the transition region of the step. As a result, the Rx beam patterns of the SRA shown in Figure 10 have flat-topped patterns with increased EOC gain. Rx beam EOC gain improvement is about 1.2 dB when compared with Configuration "C". By combining the feed phase quadratic variation and the phase variation due to the step, the step size can be minimized and the step can be blended with the reflector shape. The SRA concept works well for wide angle coverage regions and shows significant improvements in Rx gain, Rx C/I, Tx C/I and moderate improvement of Tx gain when compared to a reflector without the step(s).

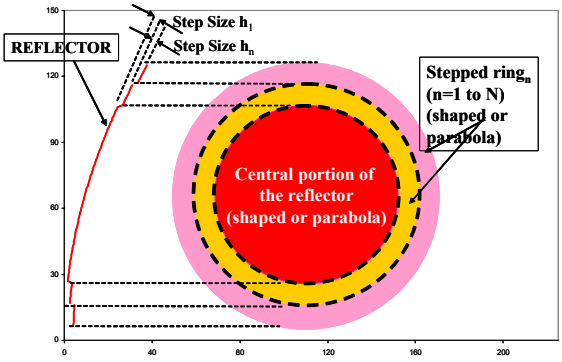

Fig. 8. Concept of "Stepped-Reflector Antenna".

c) DBS Antennas

LMCSS has developed advanced antenna payloads for direct broadcast satellites for local channel broadcast over the CONUS. These include multi-aperture reflectors with high efficiency feeds. Figure 11 shows typical coverage using multiple spot beams covering

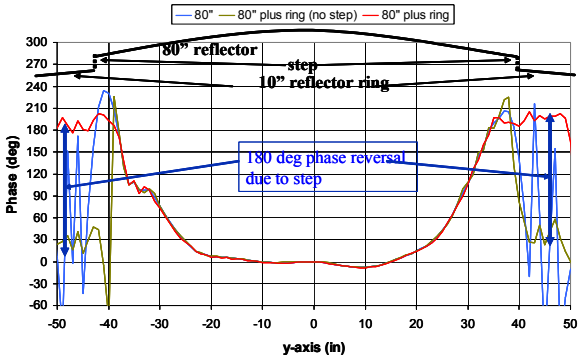

Fig. 9. Near-Field Phase Distribution of SRA.

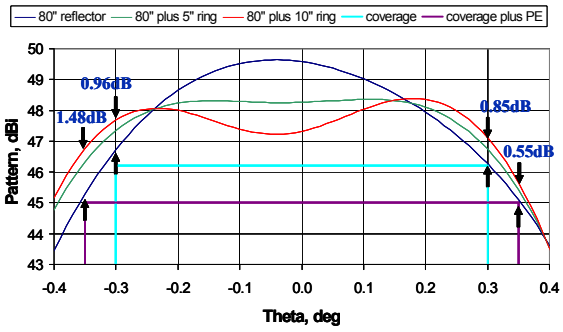

Fig. 10. Computed DMBA patterns of SRA showing "flat-topped" main beam with increased EOC gain.

designated market areas (DMAs). Key limitation for these systems is the downlink C/I performance that has significant impact on the link availability. Use of high efficiency horns and selective shaping approach to the reflectors alleviate this limitation by providing improved C/I compared to conventional antennas. Typical EIRP and aggregate C/I performance for a specific channel are shown in Figs. 12 and 13. These beams reuse the frequency channel. The aggregate C/I has improved by

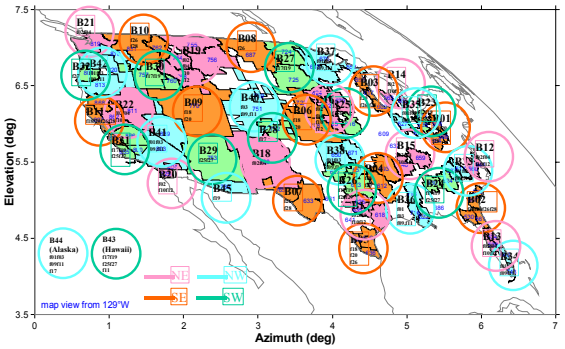

Fig. 11. DMA Coverage for a DBS Satellite.

more than 4.0 dB by employing high efficiency horns. The worst C/I performance is better than 15 dB.

d) Reconfigurable Antennas

LMCSS has been developing reconfigurable payloads for HIEO and GEO satellites using "non-focused reflector" (NFR) antennas being fed with a small active feed array [12]. Main advantages are that it minimizes the number of feed array elements required for a given coverage, and has better scan performance due to the fact that the feed array location relative to the reflector is unchanged.

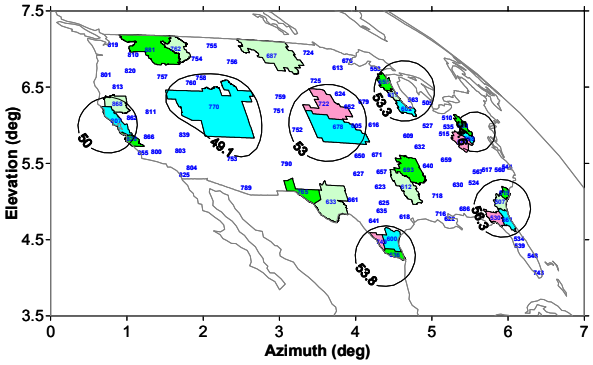

Fig. 12. EIRP Plots for the DMA Coverage of a channel.

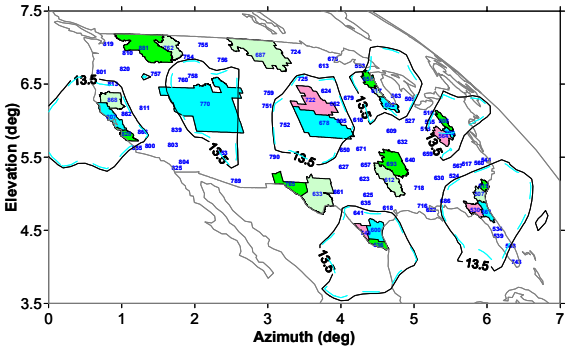

Fig. 13: Aggregate C/I Performance of the DMAs reusing the same frequency.

A quadratic phase distribution is generated by "opening-up" or "closing-in" the parent paraboloidal reflector. The NFR broadens the element beams significantly that allows reducing the number of feed array elements, when compared to a conventional parabolic reflector with de-focused feed array used for mobile satellites. The concept of NFR is illustrated in Fig. 14. Design examples of a HIEO satellite using a 37 element feed array are discussed. All the feed array elements are excited uniformly in amplitude and the relative phase excitations are varied through variable phase shifters to electronically reconfigure the beam as the satellite goes through the highly elliptical orbit. Fig. 15 shows the element beams covering CONUS and synthesized beams for different yaw angles are shown in Fig. 16. The NFR technology is applicable to both HIEO and GEO satellites and has the advantages of reconfiguring the beam for different orbital locations of the satellite and provides continuous reconfiguration of the beam at different times of the HIEO satellite.

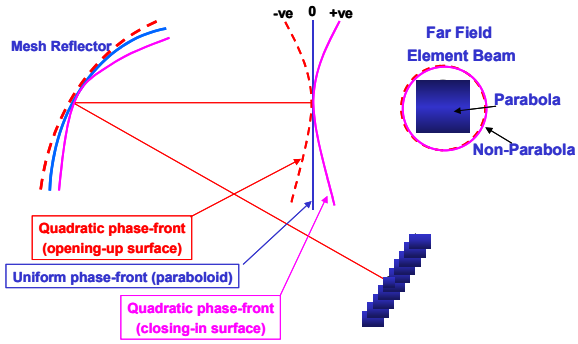

Fig. 14. NFR Concept for Reconfigurable Beam Antennas.

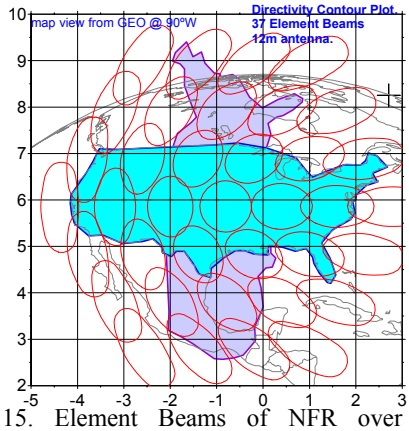

Fig. 15. Element Beams of NFR over CONUS Coverage.

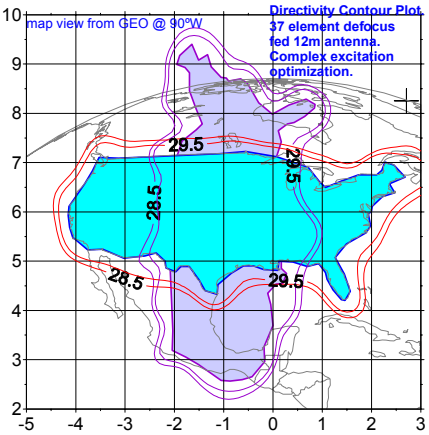

Fig. 16. Synthesized CONUS Beam of a HIEO Satellite for different Yaw angles of the satellite.

III. LENS MBAs

The lens MBAs are similar to reflector MBAs with the exception that they work on the transmission of RF signals through the lens material instead of reflection from the surface of the reflector. Because of this, lens MBAs have symmetrical geometries and are located typically on nadir deck of the spacecraft. Lenses have more degrees of freedom than reflector MBAS, but are rarely used for satellite communications due to limited bandwidth, accommodation issues on spacecraft, increased mass, and susceptibility to electro-static discharge in the case of dielectric lenses. Lens MBAs are classified into dielectric lens MBAs and waveguide lens MBAs.

a) Dielectric Lens MBAs

It was demonstrated that a thin spherical lens satisfying the Abbe sine condition, has virtually no coma lobes and therefore has wide scan properties [13, 14]. The radiated beams from such a lens are virtually invariant with scan resulting in maximum coverage gain and better sidelobe isolation among frequency re-use beams. Advantages of spherical lens are that it has very

low scan loss (< 0.7 dB over +/ 10 beamwidths of scan), ease of fabrication, and significant mass reduction (about 75%) achievable through zoning of the lens using finite steps. Surface matching of the lens is usually realized by means of circumferential slots on both surfaces of the lens. A triangular ray-tube analysis method for accurate prediction of lens antennas has been developed by Chan et al [15]. Fig. 17 shows the zoned dielectric lens using Rexolite material and designed with 5 zones. Measured radiation patterns of the lens MBA are shown in Fig. 18.

Fig. 17. Zoned Dielectric Lens Antenna at EHF.

b) Waveguide Lens MBAs

Waveguide lenses for MBA applications have been used for the DSCS program. It is very similar to the dielectric lens, except it is made up of large number of waveguide elements (circular or rectangular) with varied lengths in order to compensate for the phase variation across the lens. The waveguide lens needs to be zoned in order to minimize the mass. Because of the zoning, the bandwidth of the waveguide lens is narrow and is typically of the order 5% or less. It also suffers from gain loss due to high mutual coupling among the waveguide elements and poor return loss, but is preferred over dielectric lens MBAs for space applications. Details of the waveguide lens are given earlier [7, see Fig. 3.139 for a photograph of an X-band waveguide lens MBA].

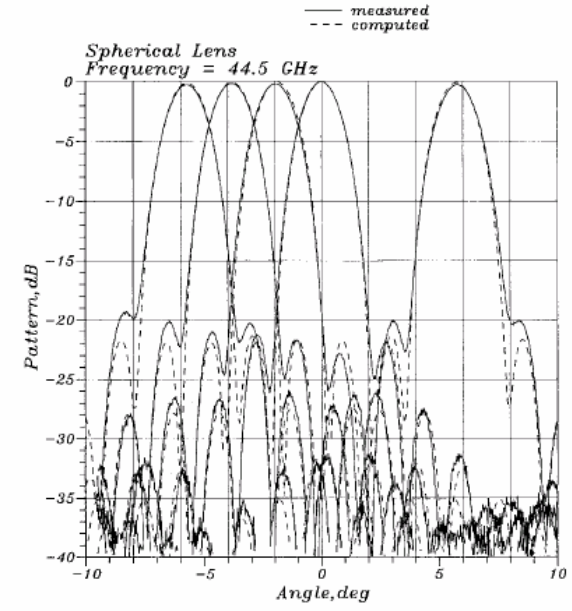

Fig. 18. Radiation Patterns of an EHF Dielectric Lens MBA.

IV. PHASED ARRAY MBAs

The phased array MBAs have been employed in the past for satellite communications requiring multiple beams. The advantage with phased array MBA is that it requires a single aperture to generate all the beams. Because of the limited bandwidth capability of phased arrays, it requires separate antennas, one for Tx and the other for Rx. These phased arrays typically employ horns as radiating elements. Array elements are arranged in either a square lattice or a hexagonal lattice. Maximum size of the element is determined by the grating lobe criteria and is given as

$$\frac{d^{S,H}}{\lambda_H} \le \frac{1.0,1.1547}{\sin\theta_G + \sin\theta_{sm}} \tag{21}$$

where θ_{sm} is the maximum scan angle over the coverage region of MBA, θ_G is the closest location of the grating lobe, λ_H is the wavelength at highest frequency of operation, and $d^{S,H}$ are the maximum size of the horn element for square and hexagonal array lattices of the array. For example, the feed horn size is about 3 wavelengths with θ_{sm} as 9 degrees and θ_G as 13 degree The element directivity is a function of the element size and the efficiency, and is given in by

$$D_e = 10\log_{10}\left[\frac{4\pi A_e}{\lambda^2}\eta_e\right] \quad \text{dBi} \tag{22}$$

where A_e is the element area, and η_e is the element efficiency which is a function of the type of the radiating element. In order to size the phased array in terms of number of elements, the scan loss of the array needs to be calculated. The scan loss is a function of element roll-off and is given in dB as

$$SL = 3\left[\frac{\theta_{sm}}{0.5\theta_3}\right]^2 \tag{23}$$

where θ_{sm} is the maximum scan angle of the coverage region and θ_3 is the half-power beam-width of the element which is given by

$$\theta_3 = A\lambda / d_e \tag{24}$$

where the constant A varies with the type of the horn and is 63, 70, 55, and 52 for high-efficiency circular horn, Potter horn, dominant-mode square or rectangular horn, and high-efficiency square/rectangular horns, respectively. The number of elements required for the array is given as

$$N = 10^{0.1(D_A - D_e)} \tag{25}$$

where D_A is the required antenna directivity to meet the desired edge-of-coverage gain of the MBA and is given as

$$D_A = G_m + X + L_S + SL + T_L + I_m \tag{26}$$

where G_m is the minimum coverage gain, X is the triple beam overlap of the MBA (typically 3 dB to 5 dB), SL is the scan loss, L_S is the antenna loss, T_L is the illumination taper loss of the array, and I_m is the implementation margin to account for gain degradation due to amplifier failures, amplitude and phase excitation errors, and thermal effects.

Fig. 19 shows typical block diagram of the phased array transmit MBA. Each of the M beams are synthesized independently using phase only synthesis with fixed amplitude distribution of the array. The desired amplitude distribution can be achieved by using SSPAs with varying RF power. The beam forming network is realized at low-level (before amplifiers) in order to minimize output losses.

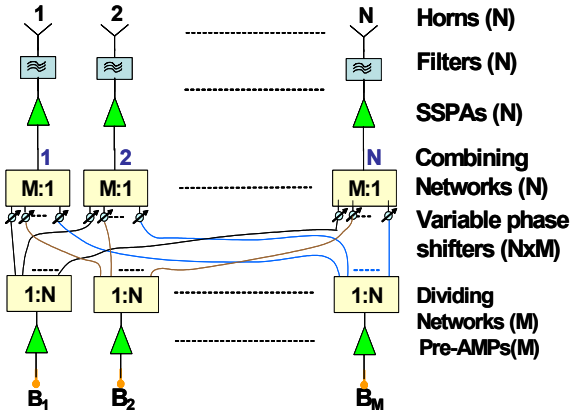

Fig. 19. Block Diagram of the Phased Array MBA.

There are a number of ways that beamforming for phased array MBAs can be realized. The block-diagram shown in Fig. 19 employs corporate BFN using couplers. This is considered suitable for most of the commercial satellite applications requiring moderate bandwidths of less than 15%. However, for wide bandwidth and multi-band applications Rotman lens BFN (Fig. 20) is widely used. The advantage of the Rotman lens BFN is that the beam locations are invariant with frequency, since it produces true-time delay response over the array. A three-dimensional

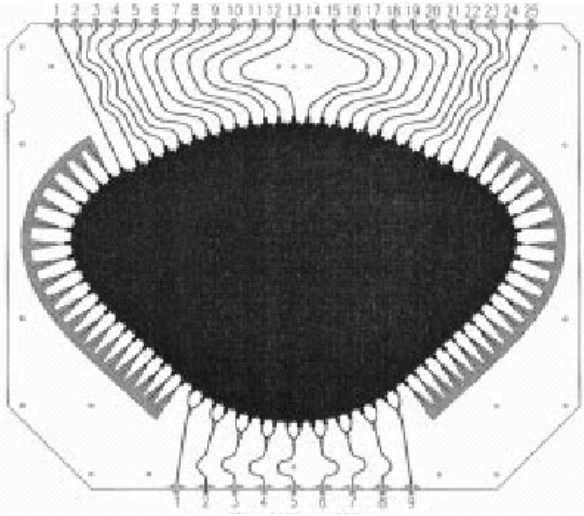

Fig. 20. Trace of a single Rotman lens with 9 beam ports and 25 array ports.

stack of row and column Rotman lenses feeding an array with hexagonal grid has been presented [16]. The number of Rotman lenses required is the maximum number of elements in a row of the array plus the maximum number of beams in a row of the coverage region. Rotman lenses can be implemented in either strip-line or microstrip medium. Dual-port excitation method for the beam ports is often employed in order to minimize the spill-over losses of the lens. Figure 20 shows the trace of a single Rotman lens with 9 beam ports and 25 array ports. The three-dimensional stack of 34 Rotman lenses feeding an array of 489 elements is shown in Fig. 21. Fig. 22 shows radiation patterns of a prototype array with Rotman lens feed network.

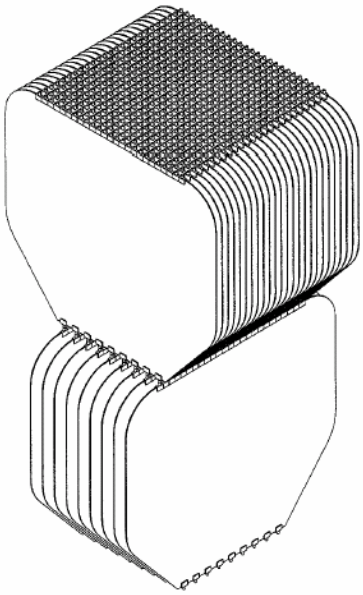

Fig. 21. Rotman Lens BFN with row and column boards.

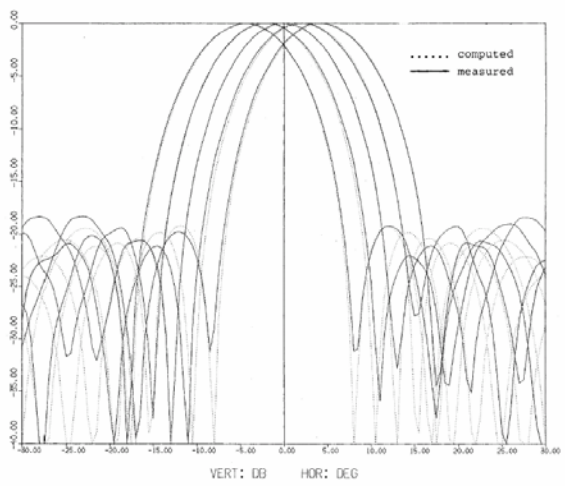

Fig. 22. Radiation Patterns of an Array Antenna with Rotman Lens BFN.

V. CONCLUSIONS

A review of multiple beam antenna technology applicable for satellite communication payloads is presented. It includes reflector MBAs, lens MBAs, and phased array MBAs. Design of MBAs, performance analysis, and hardware implementation aspects are discussed. The reflector MBAs are widely used for satellite applications due to mature technology, reduced cost, and improved performance.

REFERENCES

[1] S. Rao, G. Morin, M. Tang, and K.K. Chan, "Development of a 45 GHz Multiple-Beam Antenna for Military Satellite Communications," IEEE Trans. Antennas Propagat., Vol. 43, pp. 1036-1047, October 1995.

[2] S. Rao, "Design and Analysis of Multiple-Beam Reflector Antennas," IEEE Antennas Propagat. Magazine, Vol. 41, pp. 53-59, August 1999.

[3] S. Rao, "Parametric Design and Analysis of Multiple-Beam Reflector Antennas for Satellite Communications," IEEE Antennas Propagat. Magazine, Vol. 45, pp. 26-34, August 2003.

[4] S. Rao and Minh Tang, "Stepped-Reflector Antenna for Dual-Band Multiple Beam Satellite Communications Payloads," IEEE Trans. Antennas Propagat., Vol. 54, pp. 801-811, March 2006.

[5] S. Rao, K.K. Chan, and M. Tang, "Dual-band multiple beam antenna system for satellite communications," IEEE AP-S Symposium, Washington, DC, July 2005.

[6] O. Sotoudeh et al., "Dual-band hard horn for use in cluster-fed multi-beam antennas in Ka-band", IEEE AP-S Symposium, Washington, DC, July 2005.

[7] A. W. Rudge et al., "The Handbook of Antenna Design," Peter Peregrinus Ltd, IEE, pp. 466-505, 1986

[8] L. J. Ricardi et al., "Radiation pattern calculations for a waveguide lens multiple-beam antenna operating in the AJ mode," MIT Lincoln Laboratory Technical Note 1975-25, 1976.

[9] S. Rao et al., "Multiple beam antenna using reflective and partially-reflective surfaces," US Patent # 6,759,994 B2, July 06, 2004.

[10] S. Rao and M. Tang, "Multiple-beam antenna system using high-efficiency dual-band feed horns," US Patent Application 60/622785, October 29, 2004.

[11] S. Rao and M.Tang, "Stepped-reflector antenna system for dual-band multiple beam satellite payloads," US Patent Application 60/693832, June 27, 2005.

[12] S. Rao et al., "Reconfigurable payload using non-focused reflector antenna for HIO and GEO satellites," US Patent Application 60/758684, January 13, 2006.

[13] W. Rotman and R.F. Turner, "Wide angle microwave lens for line source applications," IEEE Antennas & Propagat., vol. 11, pp. 623-632, Novemnber 1963.

[14] D. Archer, "Lens-fed multiple beam arrays," Microwave Journal, vol. 18, pp. 37-42, 1975.

[15] K. K. Chan et al., "Triangular ray-tube analysis of dielectric lens antennas," IEEE Trans. Antennas Propagat., vol. 45, pp. 1277-1285, August 1997.

[16] K.K. Chan and S. Rao, "Design of a Rotman lens feed network to generate a hexagonal lattice of multiple beams," IEEE Trans. Antennas Propagat., vol. 50, pp. 1099-1108, August 2002.

Sudhakar K. Rao (M'83–SM'97–F'06) was born in Tenali, Andhra Pradesh, India. He received the B.Tech degree from REC Warangal, India, in 1974, the M. Tech degree from the Indian Institute of Technology, Kharagpur, in 1976, and the Ph. D degree from the Indian Institute of Technology, Madras, in 1980, all in electrical engineering. From 1976 to 1977, he worked as a Technical Officer at the Electronics Corporation of India Limited (ECIL), Hyderabd, and was involved with the design and test of LOS and TROPO communications antennas. From 1980 to 1981, he worked as a Senior Scientific Officer at the Electronics and Radar Development Establishment (LRDE), Bangalore, and worked on phased array radar antennas. During 1981 to 1982, he worked at the University of Trondheim, Norway, on a post-doctoral fellowship from the Royal Norwegian Council for Scientific and Industrial Research (NTNF). He was a Research Associate at the University of Manitoba, Winnipeg, Canada, from 1982 to 1983, where he worked on low-sidelobe antennas. From 1983 to 1996, he worked as a Staff Scientist at the Spar Aerospace Limited, Ste-Anne-de-Bellevue, Quebec, Canada on several satellite communications payloads for fixed and broadcast satellite services, mobile satellites, agile beam payloads at EHF, and led the IRAD team that developed several advanced antenna components and sub-systems that include cup-dipole arrays, lens antennas, helical antennas, phased arrays, and dual-gridded shaped reflectors. From 1996 to 2003, he worked at Hughes Satellite Communications (that later became Boeing Satellite Systems), El Segundo, CA as a Chief Scientist and developed advanced multiple beam and reconfigurable beam payloads for several commercial and military communications satellites that include Wideband Gapfiller, Anik-F2, NewSkies-8, GOES, DTV-4S, Thuraya, and GPS-2. He is currently working at Lockheed Martin Commercial Space Systems, Newtown, PA, as a Division Fellow in the payload engineering directorate. He has published over 90 technical papers in various journals and conferences in the areas of microwave antennas and satellite communications payloads and has 30 U.S. patents issued/pending. His current research interests include reconfigurable payloads, multiple beam payloads, feed assemblies, high power payload test methods, and reflector antennas.

Dr. Rao received several awards including Boeing's Technical Fellow award in 2001, Boeing's Special Invention award in 2002, BSS' Technical/Patent Excellence award in 2003, Lockheed Martin's Inventor of New Technology award in 2005, LMCSS' Special Recognition awards in 2004 & 2005, and LMCSS's Technical Excellence award in 2006. In 2006, Dr. Rao received IEEE Benjamin Franklin Key award in Philadelphia in recognition of his original contributions and innovations in the field of satellite communications. His work on modeling of satellite antenna patterns was adopted by the CCIR in 19992. Dr. Rao is an IEEE Fellow and served as the member of technical program committee for several IEEE AP-S/URSI conferences, chaired numerous technical sessions, served as the IEEE A&A Committee for Senior Member selection for Region 2, and has been serving as a reviewer for the IEEE Transactions on Antennas and Propagation since 1985.

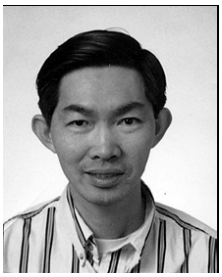

Minh Q. Tang was born in Saigon, Vietnam. He studied physics and mathematics at the University of Winnipeg, Manitoba, Canada, from 1976 to 1978. He received the B.S. degree in electrical engineering from the University of Manitoba, Manitoba, in 1981, where, from 1981 to 1982, he engaged in graduate studies. From 1983 to 1996, he worked at Spar Aerospace Limited, Ste-Anne-de-Bellevue, Quebec, Canada, as a Specialist Engineer and was involved with antenna designs for contoured beam and multiple beam payloads for both commercial and military satellites. From 1996 to 2004, he worked at Space Systems Loral, Palo Alto, CA, where he served as a Technical Consultant for the satellite antenna division. He has been with Lockheed Martin Commercial Space Systems, Newtown, PA, since 2004, where he is currently a Principal Engineer working with new business group of the Payload Engineering Division. He has published about 14 papers in technical conferences and journals and has five U.S. patents that are issued and pending. His current research interests include contoured beam antennas, reconfigurable antennas and multiple beam antennas. Mr. Tang received Lockheed Martin's Technology Award in 2005 and LMCSS' Special Recognition Award in 2005 and in 2006.

Chih-Chien Hsu was born in Taipei, Taiwan, in 1965. He received the B.S. degree in Electronics Engineering from the National Chiao-Tung University, Taiwan in 1987, and M.S. & PH.D. from Massachusetts Institute of Technology in 1992 and 1996, respectively. He has been working on antenna systems for communication and radar applications at Boeing Satellite System and Lockheed Martin Corporation for the past 10 years. Currently he is with Lockheed Martin Commercial Space System, Newtown, PA, as a Senior Staff Engineer working with new business group of the Payload Engineering Division. His current research interests are in the areas of multi-beam antenna design and phased array technology. He has four U.S. patents on antenna and communication system.